



Chiang Mai J. Sci. 2018; 45(4) : 1770-1781

<http://epg.science.cmu.ac.th/ejournal/>

Contributed Paper

Thermal and Acid Activation (TAA) of Bentonite as Adsorbent for Removal of Methylene Blue: A Kinetics and Thermodynamic Study

Tarmizi Taher [a], Dedi Rohendi [b], Risfidian Mohadi [b] and Aldes Lesbani* [a,b]

[a] Department of Environmental Science, Graduate School Sriwijaya University, Jl. Padang Selasa, No. 524, Bukit Besar, Palembang, Sumatera Selatan, Indonesia.

[b] Department of Chemistry, Faculty of Mathematic and Natural Science, Sriwijaya University, Jl. Palembang - Prabumulih KM.32 Kabupaten Ogan Ilir, Sumatera Selatan, Indonesia.

* Author for correspondence; e-mail: aldeslesbani@pps.unsri.ac.id

Received: 24 January 2017

Accepted: 14 June 2017

ABSTRACT

Natural bentonite grounded from Sarolangun District of Jambi Province has been modified based on Thermal and Acid Activation (TAA). The thermal activation was conducted by calcination at temperature 400 °C and followed by chemical activation using H₂SO₄. In order to investigate the change of the bentonite structure before and after activation process, the chemical analysis by XRF, XRD powder, BET, and FTIR was conducted. The TAA bentonite then used as an adsorbent to remove the methylene blue dye from aqueous solution by studying the kinetics and thermodynamic of the adsorption process. The result of the structural analysis showed that during the activation process, the structure of bentonite was not changed significantly and the surface area of the activated bentonite has increased from 55.6 to 75.6 m²/g. The kinetics studies of adsorption methylene blue onto TAA bentonite revealed that the adsorption process followed the pseudo-second-order kinetic equation rather than the pseudo-first order kinetics. The kinetic data obtained presented that by increasing the initial dye concentration, the adsorption speed was reduced. The thermodynamic adsorption study revealed that the adsorption process was spontaneous showed with the negative value of free Gibbs energy.

Keywords: bentonite, thermal and acid activation (TAA), methylene blue, kinetics, thermodynamic

1. INTRODUCTION

The textile industry is one of the industrial sectors that plays a major role in Indonesia's economic development. However, the raised of the textile industry also carried serious environmental problems[1]. The textile

industry generates a colored wastewater effluent as dye residue from coloring process. Commonly, dyes used in textile industry are a synthetic dye that contains a hazardous chemical and have a high chemical oxygen

demand (COD) [2]. Methylene blue, as illustrated in Figure 1, is one of the synthetic dyes that widely used in textile industry. Due to its complex chemical composition, dye contamination into water body has high toxicity to the aquatic life and even human life. Dye contamination to the aquatic ecosystem can disturb life equilibrium by blocking the light path through water and reducing the aquatic photosynthetic activity [3]. Thus, the removal of dye contaminant in wastewater becomes an interesting challenge in water treatment area.

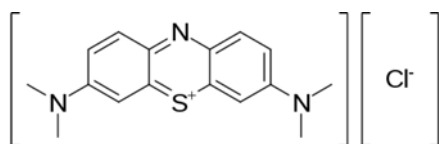


Figure 1. Chemical structure of methylene blue dye.

Lots of methods have been applied to remove dye contamination in the textile effluent. The most possible and applicable methods including chemical oxidation [4], filtration [5], ozonation [6], membrane separation [7], ion-exchange [8], microbial degradation [9], and adsorption [10]. Even each of these methods has been widely developed, all of these methods have some limitations to remove dye contamination in textile effluent completely. However, adsorption method is considered as the most cost-effective technique for dye removal from textile effluent [11].

Currently, activated carbon is the most common material used as an adsorbent in dye removal by adsorption process. The main advantage of activated carbon is due to its large surface area and high adsorption capacity [12]. However, because of its high cost, and its regeneration difficulties recently activated carbon usage

is being abandoned. As an alternative, many low-cost materials are being developed to form a powerful adsorbent material. The main source of the low-cost materials that have been widely used as an adsorbent for removal of wastewater effluent are household wastes, agricultural products, industrial wastes, sea materials, and soil and ore materials [13]. Clay as of the soil and ore mineral is an abundant natural material with low economic cost. Clay has the unique surface characteristic that made it potential to use as adsorbent material [14].

Many kinds of clay and clays minerals have been utilized as an adsorbent material in dye removal from wastewater such as zeolite [15], sepiolite [16], kaolinite [17], palygorskite [18], and bentonite [19]. Among these materials, bentonite is the largest clay mineral utilized for dye removal due to its high capability to develop and relatively high adsorption capacity. Bentonite is clay material that mainly constructed by montmorillonite minerals. It is smectite class mineral with layered structure composed by one Al octahedral sheet flanked by two silica tetrahedral sheet. Naturally, bentonite has negative surface charged due to the isomorphs substitution of Al^{3+} to Si^{4+} in the tetrahedral sheet and Mg^{2+} to Al^{3+} in the octahedral sheet [20].

In order to improve the adsorption capability of natural bentonite, some modification methods have been introduced recently including acid activation [21], thermal activation [22], cold plasma treatment [23] and pillarization [24]. The most common method of bentonite modification was by pillarization procedure. Based on the result reported by Aguiar [25], the pillarization method has significantly increased the adsorption capacity of natural bentonite. However, that method was not a simple method and need some difficult step

procedure that will reduce the time efficiency.

As an alternative of bentonite modification, the other modification methods by combining the existing method have been developed. Al-Asheh et al. [26] has been combined the chemical activation method using sodium dodecyl sulphate (SDS) followed by thermal activation at high temperature condition (850°C). The result revealed that by this combination method, the adsorption capacity of the bentonite has raised significantly toward methylene blue dye adsorption in aqueous solution. As reported by Eren and Afsin [27], the acid activation bentonite has raised the surface properties of the bentonite. Herein, bentonite modification by combination method of thermal and acid activation is a simple modification procedure that applicable to enhance the surface properties of the bentonite sample prior used as adsorbent materials.

This study is subjected to enhance bentonite adsorption capacity to the methylene blue dye by physical and chemical activation. Bentonite activation has been conducted by using two-step activation, thermal activation followed by acid activation. Herein, the activated bentonite result is used to remove methylene blue contamination in aqueous solution. Methylene blue adsorption properties, kinetic and thermodynamic, were studied by batch equilibrium methods.

2. MATERIALS AND METHODS

2.1 Chemicals and Instrumentation

Sulfuric acid (Merck) used in this study was reagent grade 96%. Natural bentonite used in this study was obtained commercially from Sarolangun District, Jambi Province, Indonesia. Bentonite sample then washed using deionized water three times and then dried at 90°C for 8 hours in an oven. Prior to use, bentonite sample was crushed

and sieved through 200 mesh ASTM standard sieve. Methylene blue M9140 dye used as a surrogate of the dye pollutant was obtained from Sigma-Aldrich Chemicals without further purification.

The chemical analysis of natural bentonite before and after activation was carried out using X-Ray Diffractometer Lab-X type 6000 with Cu-K α radiation and one deg.min⁻¹ scanning speed from 4° to 18°. The element content of the bentonite sample was analyzed by using X-ray Florescence instrument from PANanalytical type Minipal 4 under room and helium atmosphere. The functional group of natural bentonites and activated bentonite was analyzed using FTIR spectroscopy. The FTIR spectra were measured in 4000-400 cm⁻¹ wave number using Shimadzu FTIR Prestige-21 with KBr pellet. The surface area of the natural bentonite and TAA bentonite sample were measured based on BET method using N₂ physisorption isotherm in a Micromeretic apparatus. Thermal activation of the natural bentonite was conducted using Thermolyne muffle furnace from Thermo Scientific at 400 °C for 3 hours. The remaining concentration of methylene blue after adsorption was calculated using spectrophotometry technique (calibration curve method). The methylene blue absorbance measured using Uv-Vis spectrophotometer Genesys™ 20 from Thermo Scientific at 665 nm.

2.2 Methods

2.2.1 Natural bentonite activation

Natural bentonite activation was performed by a two-step procedure based on the work done by Toor et al. [28], thermal activation followed by acid activation. Thermal activation was conducted by heating the sample using muffle furnace at 400 °C for 3 hours then cooled and stored

in a desiccator for one night. The acid activation was performed using H_2SO_4 0.1 M with bentonite to acid ratio was 1:5 (g mL^{-1}). The activation process was conducted in 500 mL beaker glass equipped with magnetic stirrer. The mixture was stirred vigorously at 80°C for 3 hours. The mixture then filtered and washed several times using deionized water to remove the acid exceed. Activated bentonite then dried at 80°C for 5 hours in a laboratory oven. Dried activated bentonite was analyzed using XRF, XRD and FTIR and ready to use as an adsorbent.

2.2.2 Methylene blue solution preparation

Methylene blue stock solution (1000 mg L^{-1}) was prepared by diluting 1 g (weighed analytically) of methylene blue powder into 1000 mL of deionized water. Methylene blue standard solution ($5\text{-}200\text{ mg L}^{-1}$) was prepared by diluting the stock solution with desired concentration using deionized water. The absorbance of the standard solution was measured to make a calibration curve for measuring the methylene blue concentration after adsorption process.

2.2.3 Adsorption experiments

The adsorption experiment was performed in the batch system. All the adsorption experiments were carried out in normal pH condition, and volume of the dye solution was 50 mL. A known amount of activated bentonite adsorbent was added into methylene blue solution in 250 mL Erlenmeyer flask equipped with a magnetic stirrer. The mixture was agitated with constant speed (180 rpm) with a predetermined time. As soon as agitation process has stopped, the dye solution was separated using filtration paper. The dye concentration remained in the supernatant was calculated by using UV-Vis spectrophotometer.

The adsorption parameters that affected

the adsorption process were studied. Effect of the initial dye concentration was investigated by varying the initial dye concentration (50, 100, 150 mg L^{-1}). Effect of adsorption time was examined by varying the time of adsorption (5, 10, 15, 20, 25, 30, 45, and 60 minutes). Effect of the adsorption temperature was studied by varying the adsorption temperature at room temperature at 30, 40, and 60°C .

The amount of methylene blue adsorbed onto activated bentonite was calculated using following equation:

$$q_t = \frac{(C_0 - C_t)V}{m} \quad (1)$$

Where q_t , C_0 , C_t , V , and m are amount of methylene blue adsorbed per gram of activated bentonite at any time t (mg L^{-1}), initial methylene blue concentration (mg L^{-1}), concentration of methylene blue at t time adsorption (mg L^{-1}), Volume of methylene blue used (L), and amount of adsorbent used (g).

3. RESULT AND DISCUSSION

3.1 Activated Bentonite Characterization

3.1.1 X-ray fluorescence (XRF) analysis

X-ray fluorescence (XRF) spectrometer is one of the X-Ray instrument that commonly used to analyze the chemical composition of the inorganic minerals such as rock, sediment, and also clays materials [29]. The XRF analysis result of the natural bentonite sample and TAA bentonite sample were shown in Table 1. The major constituent of the natural bentonite used in this study was SiO_2 and Al_2O_3 and other impurities oxide such as Fe_2O_3 . The ratio of $\text{SiO}_2:\text{Al}_2\text{O}_3$ was found as 2.56 indicate that the natural bentonite used in this study contain montmorillonite mineral [19]. After the thermal and acid activation, the fraction of Al_2O_3 was decrease but otherwise, the SiO_2

was increased. The decreasing of the Al^{3+} content during the activation process due to the dissolution of the minerals by acid activation [21]. The Ti^{4+} fraction after activation process also relatively increased. The increasing of the TiO_2 due to the location Ti^{4+} fraction was on either octahedral or tetrahedral site [30].

Table 1. Chemical composition of natural bentonite and TAA bentonite based on XRF analysis.

| Composition | Natural bentonite (%mass) | TAA Bentonite (%mass) |
|-------------|---------------------------|-----------------------|
| SiO_2 | 43.6 | 47.5 |
| Al_2O_3 | 17 | 14 |
| TiO_2 | 1.87 | 1.96 |
| Fe_2O_3 | 33.39 | 34.28 |
| NiO | 0.87 | 0.86 |
| CaO | 0.99 | 0.44 |
| P_2O_5 | 0.71 | 0.67 |
| K_2O | 0.2 | 0.09 |
| MnO | 0.12 | 0.14 |

3.1.2 BET surface area analysis

The surface area of natural bentonite and TAA bentonite has been measured based on the N_2 physisorption isotherm studies. Figure 2 shows the N_2 physisorption isotherm properties of natural and TAA bentonite sample. All the curve presented indicated that the isotherm properties of the sample were type II isotherm [31]. The measurement of the specific BET surface area, total pore volume, and average pore diameter was conducted using standard BET method and the BJH equation. Table 2 show that the TAA bentonite has larger surface area than natural bentonite. As reported by Pawar et al. [32], the increase of the surface area of the TAA bentonite due to the particles within dissolved octahedral sheet were splitted.

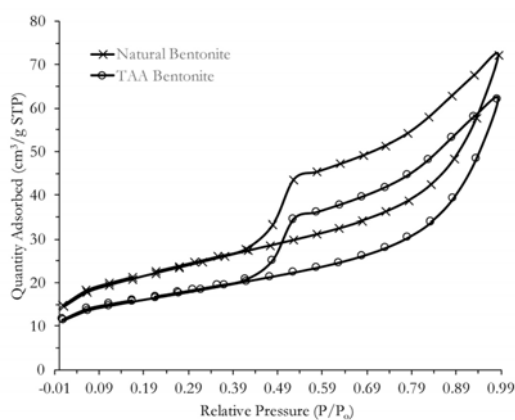


Figure 2. N_2 Physisorption isotherm of natural bentonite and TAA bentonite.

Table 2. Surface area, total pore volume, and pore diameter of natural and TAA bentonite.

| Materials | BET surface area (m^2/g) | Total pore volume (cm^3/g) | Average pore diameter (nm) |
|-------------------|------------------------------|--------------------------------|----------------------------|
| Natural Bentonite | 55.635 | 0.0959 | 6.871 |
| TAA Bentonite | 75.671 | 0.1118 | 5.911 |

3.1.2 X-ray diffraction (XRD) analysis

X-ray powder diffraction (XRD) is a well-known technique used in order to monitor the change of layer spacing of clay minerals [33]. In this study, the change of bentonite structure during the thermal and acid activation was overseen by using XRD powder technique. The XRD powder pattern of natural bentonite and activated bentonite samples were illustrated in Figure 3. Bentonite is the one of the smectite group that mainly constructed by montmorillonite mineral [34]. Based on Figure 3, the main characteristic of the smectite (montmorillonite) peak was recorded at 2θ value at about 5° , 20° and 35° [35]. The other constituent of the smectite phase including quartz recorded at 2θ about 22° and 26° and feldspar was also recorded at 2θ value about 28° [22].

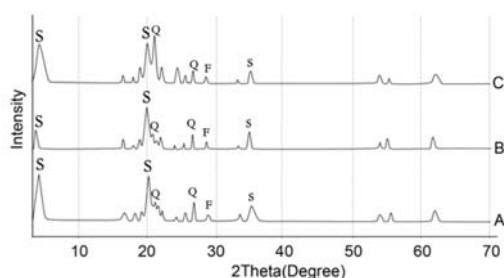


Figure 3. XRD Pattern of natural bentonite (A), thermal activated bentonite (B), and thermal and acid activated (TAA) bentonite (C) where S = smectite, Q = Quartz, and F = feldspar.

The thermal activation bentonite XRD pattern was not different significantly according to natural bentonite pattern. The appearance of these pattern differs only at the montmorillonite pattern at 2θ value about 5° . The decrease of the montmorillonite peak of the thermal activated bentonite due to the removal of the water content in the interlayer of the montmorillonite during the calcination process. The XRD powder pattern of the TAA bentonite appeared an increasing of the montmorillonite peak at 2θ about 5° compared with thermal activated bentonite pattern. That phenomenon due to the impurities in the layered structure of the smectite was partially destroyed [30]. The increasing of the montmorillonite peak also indicated that the crystallinity of TAA bentonite was excessively affected during the acid activation process [21].

As depicted in Figure 3, the diffraction peak at 22° was disappeared after acid activation process. Based on the work reported by Önal et al., [21] the diffraction peak at about 22° was indicated the present of the Opal-CT (OCT) as the impurities. In this case, Opal-CT is paracrystalline silica

($\text{SiO}_2 \cdot n\text{H}_2\text{O}$) or semicrystalline minerals that not exactly crystallized. After the activation process, the diffraction peak of the opal-CT was disappeared indicate that the acid activation process dissolved paracrystalline silica impurities.

3.1.3 FT-IR analysis

To assist the identification of contained mineral in natural bentonite and its change after thermal and acid activation, the FTIR analysis was conducted in the range of 4000 cm^{-1} to 400 cm^{-1} . The FTIR spectrum as the result of FTIR analysis of natural bentonite and activated bentonite were illustrated in Figure 4. As was described in XRF analysis result, the main fraction of the natural bentonite used was Al_2O_3 and SiO_2 . The main characteristic band of the natural bentonite spectrum (Figure 4A) indicates the present of Al-OH-Al stretching and Al-OH-Al bending at wavenumber 3626 cm^{-1} and 910 cm^{-1} respectively. The existing of the Si-O-Si stretching vibration observed as strong band at wavenumber 1033 cm^{-1} . The strong band at 3448 cm^{-1} and 1635 cm^{-1} indicate the existence of the H-O-H stretching and H-O-H bending respectively [36–38].

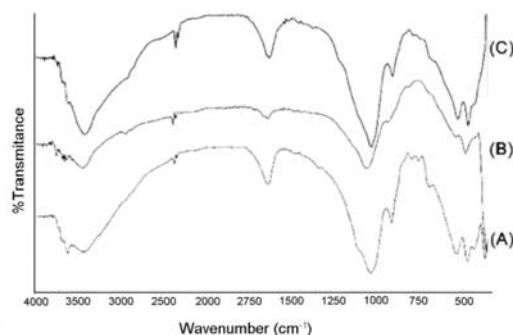


Figure 4. FTIR spectra of natural bentonite (A), thermal activated bentonite (B), and thermal and acid activated bentonite (C).

3.2 Adsorption Studies

3.2.1 Adsorption kinetic studies

The effect of contact time to the adsorption of methylene blue onto TAA bentonite was describe Figure 5. The graphic showed that the adsorption process was fast adsorption in first 10 minutes' adsorption times and then gradually slower until approached the equilibrium at 40 minutes. That phenomenon indicates that in the early stages adsorption, the numerous active site of TAA bentonite were available and by time increasing the available site to accommodate the methylene blue molecule was decreased. Similar to the contact time, by increasing the initial dye concentration the adsorption capacity of the methylene blue on TAA bentonite was gradually increased due to the increasing the driving force of the methylene blue concentration gradient to occupied the TAA bentonite active site [39].

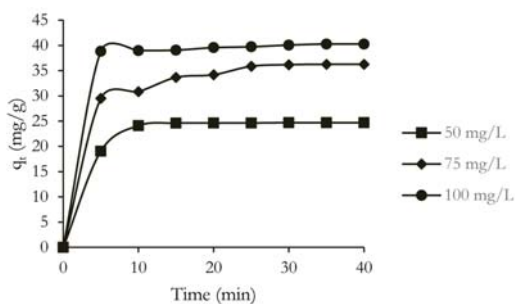


Figure 5. Effect of contact time to the adsorption capacity of methylene blue onto TAA bentonite.

Kinetics parameter is one of the important aspects in the study of dye removal by adsorption technique. The kinetic parameter is used to describe the adsorption process pathway. Kinetic parameter also reveals the dependence of physical and or chemical adsorption characteristics. Several kinetic models have been applied in order to investigate the adsorption

mechanism including, chemical reaction, diffusion control and also mass transfer [40].

Pseudo-first order model

Kinetic adsorption model by Pseudo-first order model is determined by following equation[41]:

$$\log(q_t - q_e) = \log q_e - \frac{k_1}{2.303} t \quad (2)$$

Where q_t and q_e are the amount of methylene blue adsorbed onto TAA bentonite at time t and at equilibrium. k_1 is the rate constant of methylene blue adsorption (min^{-1}). Adsorption rate constant can be determined as slop value from plot of $\log(q_t - q_e)$ versus t . If plot of versus t provide a straight line, its mean that the adsorption process is obeyed the pseudo-first order kinetic models.

Pseudo-second order model

The pseudo-second order of kinetic model is used if the pseudo-first order kinetic model was not fit enough to modeling the adsorption process. The pseudo-second-order kinetic model is represented as follows:

$$\frac{t}{q_t} = \frac{1}{k_2 q_e^2} + \frac{1}{q_e} t \quad (3)$$

Where k_2 is the rate constant of pseudo-second order (g/mg.min). By plotting t/q against t , the rate constant of pseudo-second order kinetic model is obtained by its slope value. The pseudo-second-order kinetic model is applicable to the adsorption of methylene blue onto TAA bentonite if the plot provides the straight line.

The plot of $\log(q_e - q_t)$ vs t for the first-order adsorption kinetic and the plot of t/q_t against t for the second-order kinetics model were illustrated in Figure 6 and Figure 7 respectively. These pictures describe that the adsorption kinetics of the methylene blue

onto TAA bentonite was following the pseudo-second order kinetic model. It showed by the R^2 value of the linear regression equation of both kinetic model. R^2 value of the first-order kinetic deviate from the unity value whereas the R^2 value of the second-order kinetic model fit enough to the unity value and prove straight line.

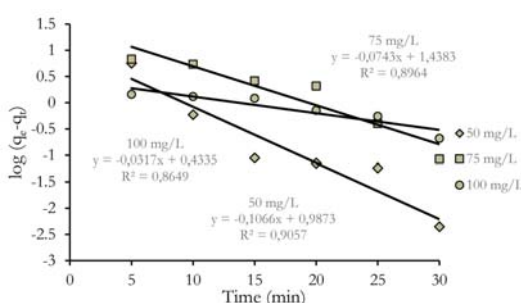


Figure 6. The first order Pseudo kinetics adsorption of congo red onto TAA bentonite in various initial dye concentration.

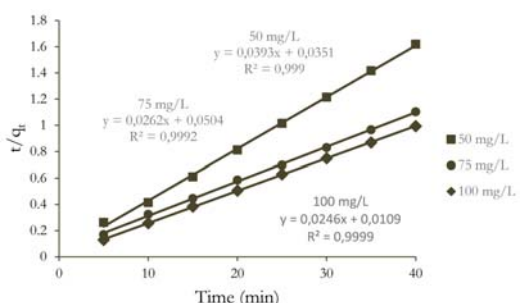


Figure 7. The second order Pseudo kinetics adsorption of methylene blue onto TAA bentonite in various initial dye concentration.

The kinetic parameter including rate constant (K) and R^2 value of both kinetic model were described in Table 3. Based on the table data, by increasing the initial methylene blue concentration, the adsorption rate constants were reduced gradually. This phenomenon can be described due to the increase of the dye concentration, the solution condition was automatically

saturated with the methylene blue molecule that can decrease the reactivity of the TAA bentonite active site [42].

Table 3. Kinetics parameter for adsorption of methylene blue on TAA bentonite.

| Initial Dye Concentration (mg/L) | K_1 (min^{-1}) | R_1^2 | K^2 (g/(mg.min)) | R_2^2 |
|----------------------------------|----------------------|---------|--------------------|---------|
| 50 | 0.245 | 0.9057 | 0.044 | 0.999 |
| 75 | 0.171 | 0.896 | 0.013 | 0.9992 |
| 100 | 0.073 | 0.864 | 0.005 | 0.999 |

3.2.2 Adsorption thermodynamic

During the adsorption process, adsorption mechanism is one of the common parameter that essential to be studied. Either the adsorption process is physical adsorption or chemical adsorption. In physical adsorption process, the interaction between the molecules relatively weak such as Van der Waals force, whereas in chemical adsorption the transfer electron mechanism might be occurred between the adsorbent and adsorbate to produce a strong chemical bond [43]. Both adsorption mechanism can be recognized based on thermodynamic parameter including the change of Gibbs free energy (ΔG°), enthalpy change (ΔH°), and entropy change (ΔS°).

These thermodynamic parameters can be measured based on the thermodynamic laws by using the following equations:

$$\Delta G^\circ = -RT \ln K_d \tag{4}$$

$$\ln K_d = \frac{\Delta H^\circ}{RT} + \frac{\Delta S^\circ}{R} \tag{5}$$

$$K_d = \frac{q_e}{C_e} \tag{6}$$

Where K_d was the equilibrium constant, C_e was the equilibrium concentration

(mgL^{-1}), q_e was equilibrium concentration of solid phase (mg. g^{-1}). R and T were the universal gas constant and absolute temperature (K) respectively. The value of the thermodynamic parameter, ΔH° and ΔS° , can be obtained as slope and intercept value from the plot $\ln K_d$ against $1/T$ respectively.

The plot of $\ln K_d$ against $1/T$ from the experiment result produced a straight enough line with R^2 value 0.911 (Figure 8). The ΔG° and ΔS° value as the slope and intercept from the linear equation obtained were computed in Table 4. It was reported that in physical adsorption, the heat involved during the adsorption process is basically at the same level with the heat of condensation process that equal to 2-20 kJ mol^{-1} . Whereas in chemical adsorption the heat involved during the adsorption process is in the range of 80 - 200 kJ mol^{-1} . In this study, the ΔH

value of the methylene blue adsorption into TAA bentonite was about 70 kJ mol^{-1} . Its value are greater than 20 kJ mol^{-1} but less than 80 kJ mol^{-1} . From this point, we assume that the adsorption process of methylene blue onto TAA bentonite was physical adsorption but tend toward chemical adsorption. In term of spontaneity, the value of ΔG° was negative in all temperature conditions but the ΔH° value was positive. It indicates that the adsorption process of methylene blue on TAA bentonite was spontaneous in the range of temperature used with endothermic characteristic [44]. Furthermore, by increasing the adsorption temperature from 303 K to 323 K, the ΔG° value was reduced, showing that the adsorption process would be favorable in higher temperature conditions.

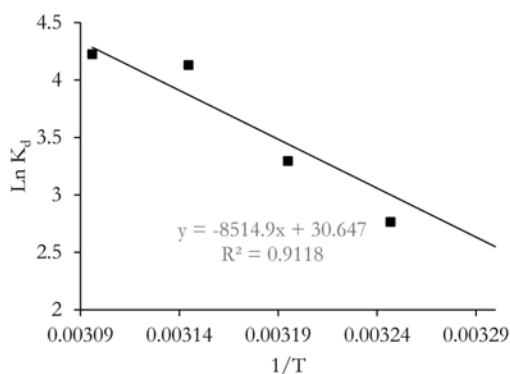


Figure 8. Plot $\ln K_d$ vs $1/T$.

Table 4. Thermodynamic adsorption parameter of methylene blue onto TAA bentonite.

| ΔH° (kJ mol^{-1}) | ΔS° (kJ (mol K)^{-1}) | ΔG° (kJ mol^{-1}) | | |
|---|---|---|--------|---------|
| | | 303 K | 313 K | 323 K |
| 70.792 | 0.254 | -6.393 | -8.941 | -11.488 |

4. CONCLUSION

The activation of natural bentonite by thermal and acid activation was successfully applied as an adsorbent material for removal of methylene blue in aqueous solution. The kinetics study of the methylene blue onto TAA bentonite show that the process follows the second-pseudo kinetics model rather than first-order kinetic model. The thermodynamic adsorption study revealed that the adsorption mechanism of the methylene blue onto TAA bentonite was physical adsorption with endothermic properties.

ACKNOWLEDGEMENT

TT thank to the Ministry of Research and Higher Education of Republic Indonesia for the financial support of this research through the *Program Magister Menuju Doktor untuk Sarjana Unggul* (PMDSU) batch II grant with contract number 326/SP2H/LT/DPRM/IX/2016 and to Integrated Research Laboratory Graduate School Sriwijaya University for the technical supporting this research.

REFERENCES

- [1] Gök Ö., Özcan A.S. and Özcan A., *Appl. Surf. Sci.*, 2010; **256**: 5439-5443. DOI 10.1016/j.apsusc.2009.12.134.
- [2] Bhatt A.S., Sakaria P.L., Vasudevan M., Pawar R.R., Sudheesh N., Bajaj H.C. and Mody H.M., *RSC Adv.*, 2012; **2**: 8663. DOI 10.1039/c2ra20347b.
- [3] Bellir K., Bouziane I.S., Boutamine Z., Lehocine M.B. and Meniai A.H., *Energy Procedia*, 2012; **18**: 924-933. DOI 10.1016/j.egypro.2012.05.107.
- [4] Navarro P., Gabaldón J.A. and Gómez-López V.M., *Dyes Pigm.*, 2017; **136**: 887-892. DOI 10.1016/j.dyepig.2016.09.053.
- [5] Liu M., Chen Q., Lu K., Huang W., Lü Z., Zhou C., Yu S. and Gao C., *Sep. Purif. Technol.*, 2017; **173**: 135-143. DOI 10.1016/j.seppur.2016.09.023.
- [6] Hu E., Shang S., Tao X., Jiang S. and Chiu K., *J. Clean. Prod.*, 2016; **137**: 1055-65. DOI 10.1016/j.jclepro.2016.07.194.
- [7] Puspasari T. and Peinemann K.V., *J. Water Process Eng.*, 2016; **13**: 176-182. DOI 10.1016/j.jwpe.2016.08.008.
- [8] Darmograi G., Prelot B., Geneste A., De Menorval L.C. and Zajac J., *Colloids Surf. A Physicochem. Eng. Asp.*, 2016; **508**: 240-250. DOI 10.1016/j.colsurfa.2016.08.063.
- [9] Fang Z., Song H., Yu R. and Li X., *Ecol. Eng.*, 2016; **94**: 455-463. DOI 10.1016/j.ecoleng.2016.06.020.
- [10] Zhang F., Chen X., Wu F. and Ji Y., *Colloids Surf. A Physicochem. Eng. Asp.*, 2016; **509**: 474-483. DOI 10.1016/j.colsurfa.2016.09.059.
- [11] Wang L. and Wang A., *J. Hazard. Mater.*, 2008; **160**: 173-180. DOI 10.1016/j.jhazmat.2008.02.104.
- [12] Khanday W.A., Marrakchi F., Asif M. and Hameed B.H., *J. Taiwan Inst. Chem. Eng.*, 2017; **70**: 32-41. DOI 10.1016/j.jtice.2016.10.029.
- [13] Ali I., Asim M. and Khan T.A., *J. Environ. Manage.*, 2012; **113**: 170-183. DOI 10.1016/j.jenvman.2012.08.028.
- [14] Hu Q.H., Qiao S.Z., Haghseresht F., Wilson M.A. and Lu G.Q., *Ind. Eng. Chem. Res.*, 2006; **45**: 733-738. DOI 10.1021/ie050889y.
- [15] EL-Mekkawi D.M., Ibrahim F.A. and Selim M.M., *J. Environ. Chem. Eng.*, 2016; **4**: 1417-1422. DOI 10.1016/j.jece.2016.01.007.

- [16] Santos S.C.R. and Boaventura R.A.R., *J. Environ. Chem. Eng.*, 2016; **4**: 1473-1483. DOI 10.1016/j.jece.2016.02.009.
- [17] Gao W., Zhao S., Wu H., Deligeer W. and Asuha S., *Appl. Clay Sci.*, 2016; **126**: 98-106. DOI 10.1016/j.clay.2016.03.006.
- [18] Al-Futaisi A., Jamrah A. and Al-Hanai R., *Desalination*, 2007; **214**: 327-342. DOI 10.1016/j.desal.2006.10.024.
- [19] Chinoune K., Bentaleb K., Bouberka Z., Nadim A. and Maschke U., *Appl. Clay Sci.*, 2016; **123**: 64-75. DOI 10.1016/j.clay.2016.01.006.
- [20] Anirudhan T.S. and Ramachandran M., *Process Saf. Environ. Prot.*, 2015; **95**: 215-225. DOI 10.1016/j.psep.2015.03.003.
- [21] Önal M. and Sarikaya Y., *Powder Technol.*, 2007; **172**: 14-18. DOI 10.1016/j.powtec.2006.10.034.
- [22] Gong Z., Liao L., Lv G. and Wang X., *Appl. Clay Sci.*, 2016; **119**: 294-300. DOI 10.1016/j.clay.2015.10.031.
- [23] Yavuz Ö. and Saka C., *Appl. Clay Sci.*, 2013; **85**: 96-102. DOI 10.1016/j.clay.2013.09.011.
- [24] Zhang Y., Li Y., Li J., Sheng G., Zhang Y. and Zheng X., *Chem. Eng. J.*, 2012; **185-186**: 243-249. DOI 10.1016/j.cej.2012.01.095.
- [25] Aguiar J.E., Bezerra B.T.C., Siqueira A.C.A., Barrera D. and Sapag K., *Sep. Sci. Technol.*, 2014; **49**: 37-41. DOI 10.1080/01496395.2013.862720.
- [26] Al-Asheh S., Banat F. and Abu-Aitah L., *Adsorpt. Sci. Technol.*, 2003; **21**: 451-462. DOI 10.1260/026361703769645780.
- [27] Eren E. and Afsin B., *J. Hazard. Mater.*, 2009; **166**: 830-835. DOI 10.1016/j.jhazmat.2008.11.132.
- [28] Toor M., Jin B., Dai S. and Vimonses V., *J. Ind. Eng. Chem.*, 2015; **21**: 653-661. DOI 10.1016/j.jiec.2014.03.033.
- [29] Jenkins R., X-Ray Diffraction; in Jenkins R., eds. *XRay Fluorescence Spectrometry*, John Wiley & Sons, Inc., Hoboken, NJ, USA, 2012: 37-51.
- [30] Tahar T., Mohadi R., Rohendi D. and Lesbani A., *AIP Conf. Proc.*, 2017; **1823**. DOI 10.1063/1.4978101.
- [31] Banković P., Milutinović-Nikolić A., Mojović Z., Jović-Jovičić N., Zunić M., Dondur V. and Jovanović D., *Appl. Clay Sci.*, 2012; **58**: 73-78. DOI 10.1016/j.clay.2012.01.015.
- [32] Pawar R.R., Lalhmunsiamma Bajaj H.C. and Lee S.M., *J. Ind. Eng. Chem.*, 2016; **34**: 213-223. DOI 10.1016/j.jiec.2015.11.014.
- [33] Sadik F., Fincher J.H. and Hartman C.W., *J. Pharm. Sci.*, 1971; **60**: 916-918. DOI 10.1002/jps.2600600624.
- [34] Choo K.Y. and Bai K., *Appl. Clay Sci.*, 2016; **126**: 153-159. DOI 10.1016/j.clay.2016.03.010.
- [35] Bankovic P., Milutinovic-Nikolic A., Jovic-Jovicic N., Dostanic J., Cupic Z., Loncarevic D., and Jovanovic D., *Proceeding tenth Annu. Conf. Mater. Res. Soc.*, Serbia, 2009; 811-815.
- [36] Yaming L., Mingliang B., Zhipeng W., Run L., Keliang S. and Wangsuo W., *J. Taiwan Inst. Chem. Eng.*, 2016; **62**: 104-111. DOI 10.1016/j.jtice.2016.01.018.
- [37] Kordouli E., Bourikas K., Lycourghiotis A. and Kordulis C., *Catal. Today*, 2015; **252**: 128-135. DOI 10.1016/j.cattod.2014.09.010.
- [38] Kalmár J., Lente G. and Fábrián I., *Dyes Pigm.*, 2016; **127**: 170-178. DOI 10.1016/j.dyepig.2015.12.025.

- [39] Liu S.Y., Gao J., Qu B., Yang Y.J. and Xin X., *Waste Manag. Res.*, 2010; **28**: 748-753. DOI 10.1177/0734242X09346976.
- [40] Bulut E., Özacar M. and Şengil İ.A., *J. Hazard. Mater.*, 2008; **154**: 613-622. DOI 10.1016/j.jhazmat.2007.10.071.
- [41] Zaghouane-Boudiaf H., Boutahala M., Sahnoun S., Tiar C. and Gomri F., *Appl. Clay Sci.*, 2014; **90**: 81-87. DOI 10.1016/j.clay.2013.12.030.
- [42] Taher T. and Lesbani A., *Srivijaya J. Environ.*, 2016; **1**: 1-4. DOI 10.22135/sje.2016.1.1.1-4.
- [43] Mahmoud M.E., Nabil G.M., El-Mallah N.M. and Bassiouny H.I., *J. Ind. Eng. Chem.*, 2016; **37**: 156-167. DOI 10.1016/j.jiec.2016.03.020.
- [44] Al-Rashed S.M. and Al-Gaid A.A., *J. Saudi Chem. Soc.*, 2012; **16**: 209-215. DOI 10.1016/j.jscs.2011.01.002.